



Cite this: DOI: 10.1039/c7cp01949a

Lifshitz phase: the microscopic structure of aqueous and ethanol mixtures of 1,*n*-diols

Martina Požar^{ab} and Aurélien Perera *^a

We study binary mixtures of ethylene glycol and 1,3-propanediol with water or ethanol using computer simulations. Despite strong hydrogen bonding tendencies between all these molecules, we find that these mixtures are surprisingly homogeneous, in contrast to the strong micro-heterogeneity found in aqueous ethanol mixtures. The aqueous diol mixtures are found to be close to ideal mixtures, with near-ideal Kirkwood–Buff integrals. Ethanol–diol mixtures show weak non-ideality. The origin of this unexpected randomness is due to the fact that the two hydrogen bonding hydroxyl groups of the 1,*n*-diol are bound by the neutral alkyl bond, which prevents the micro-segregation of the different types of hydroxyl groups. These findings suggest that random disorder can arise in the presence of strong interactions – in contrast to the usual picture of random disorder due to weak interactions between the components. They point to the important role of molecular topology in tuning concentration fluctuations in complex liquids. We propose and justify herein the name of Lifshitz phases to designate such types of disordered systems.

Received 27th March 2017,
Accepted 9th May 2017

DOI: 10.1039/c7cp01949a

rsc.li/pccp

1 Introduction

The concept of the Lifshitz point was initially pointed out in a field theoretic context,¹ as a triple point along the lambda-line separating a disordered phase from two types of ordered phases. The peculiarity of this Lifshitz point is the emergence of a characteristic $k \neq 0$ wave vector pre-peak in the scattering function $I(k)$, as one goes from the disordered phase, where the peak is at $k = 0$, to one of the ordered phases.¹ A particular property in the context of the Lifshitz point is that the transition between the disordered and the ordered phase is continuous, without the usual expected gap.¹ The emergence of a $k \neq 0$ pre-peak in this particular context is usually a sign of some sort of a layered phase. This situation is often met in the context of micro-emulsions,^{2,3} when going from the disordered phase to the lamellar phase.⁴ This type of scenario is well captured by various lattice models⁵ and their field theoretic formulations.^{3,6,7} To understand the importance of the absence of a gap, one can picture the isotropic to the layered smectic phase transition in lyotropic liquid crystals,⁸ which is always separated by a density jump, just like the liquid–solid transition, and this is in sharp contrast to conditions for the existence of a Lifshitz point. The fact that one can go continuously (without gap)

from the disordered phase to the layered phase, imposes some constraints on the type of the underlying molecular organisation, in particular, the existence of stable cluster phases,⁹ which are intermediate states between fully disordered and fully layered phases, such as raft-phases, for example. The lambda-line³ often separates the disordered phase from this cluster phase. This way, when going from the disordered phase to the layer phase, the small wave vector part of the scattered intensity increases first, due to the fluctuation of cluster formation, and then, instead of diverging as in the case of an orientational ordering, the small wave vector part of the scattered intensity increases to a non-zero pre-peak, witnessing the layer ordering. In short, the Lifshitz point implicitly requires some form of microscopic clustering to exist. However, the question of the requirement for implicit clustering in a Lifshitz point context remains ill-documented and unanswered. It seems to be a byproduct of the microscopic interactions or theoretical formulations. It is through this question that we would like to re-examine here the concept of the Lifshitz point.

In the present paper, we propose to extend this concept of the Lifshitz point to that of the Lifshitz state. The context for such a proposition is the following. In recent works,¹⁰ we have emphasized the specific nature and structural properties of the hydrogen bonding induced clustering in the context of various binary mixtures, such as aqueous,^{11–13} and non-aqueous^{14,15} mixtures and ionic liquids.^{16–19} In particular, we have demonstrated, through extensive computer simulations, that the atom–atom pair correlation functions $g_{ab}(r)$ of the clustering species tend to show long range domain oscillations, which in turn produce a domain pre-peak in the corresponding atom–atom

^a Laboratoire de Physique Théorique de la Matière Condensée (UMR CNRS 7600), Université Pierre et Marie Curie, 4 Place Jussieu, Paris cedex 05, F75252, France. E-mail: aup@lptmc.jussieu.fr

^b Department of Physics, Faculty of Sciences, University of Split, Ružera Boškovića 37, 21000, Split, Croatia

structure factors $S_{ab}(k)$, where a and b designate specific atoms in molecular species. The presence of such a pre-peak is the principal reason we proposed to designate as “molecular emulsion” all systems exhibiting this structural property.^{10,20} This is in analogy with micro-emulsion systems, which have a pre-peak in the scattered intensity $I(k)$.²¹ Unlike micro-emulsions, which exhibit various types of micellar phases, as well as lamellar phases, molecular emulsions are essentially disordered phases. It is then highly unlikely that they would possess a Lifshitz point. However, molecular emulsions and micro-emulsions share a common feature, they are both cluster based phases, with common hydrogen bonding based hydrophilic/hydrophobic characteristics at the molecular level. Therefore, they both share the clustering feature from the disordered side of the phases. As we will show here, the domain pre-peak in $S_{ab}(k)$ can disappear in certain types of mixtures, such as aqueous and non-aqueous mixtures of diols. Since both types of mixtures contain the same microscopic ordering feature, namely the hydrogen bonding ability, which is at the root of the clustering in molecular and micro-emulsions, one may wonder what would be the origin of this difference. We interpret the absence of a pre-peak in $S_{ab}(k)$ as a signature of the Lifshitz state, where the system is stuck in a disorder without clustering, but which is not a random disorder either, precisely because of the strong hydrogen bonding tendencies. From this point of view, the Lifshitz state represents a novel form of disorder, intermediate between pure random disorder and domain order, in a globally disordered homogeneous liquid. It is one step further to classify different forms of disorder in liquids, which could be of importance in classifying different types of disorder, particularly in the context of soft and bio-matter.

This study is motivated by our recent computer simulations of several pure *n*-diols,²² where we found that, despite an apparent clustering of the hydroxyl groups, which produced chain-like clusters, and a subsequent pre-peak in the oxygen–oxygen structure factors, the calculated X-ray scattering intensities showed only a weak sign of the usual cluster pre-peak found in scattering experiments of mono-ols.^{23–25} This feature was traced back to the fact that the scattering contributions of the methyl groups of linking alkyl chains produced a variety of intermediate pre-peaks, which tend to overcome the contributions of the hydroxyl groups in the summed total contribution to X-ray scattering.²² In other words, the alkyl chains linking the hydrogen bonding hydroxyl endgroups tend to produce an effective disorder, despite a strong hydrogen binding order. How does this disorder–order conflict, typical of these *n*-diols, get affected under mixing with other hydrogen bonding species? We find that it is this conflict, which gives rise to a special form of disorder that we call the Lifshitz state. This is the principal reason we have focused our study on linear 1,*n*-diols. For example, branched diols such as 1,2-propandiol, having one side with strong hydrogen bonding and a non-bonding tail, are likely to produce the same type of domain segregation as 1-propanol or t-butanol in water mixtures, hence molecular emulsions with a domain segregated pre-peak.

Ethanediol, also called ethylene glycol in the literature, has been extensively studied in aqueous mixtures, but less in alcohol and ethanol mixtures. The literature on higher diols is equally scarce. Thermodynamic studies,^{26,27} diffusion,²⁸ viscosity²⁹ as well as surface tension³⁰ measurements seem to indicate less clustering than in aqueous mono-ol mixtures. The measure of preferential solvation through the Kirkwood–Buff integrals by Y. Marcus³¹ shows the near ideality of the mixtures of 1,*n*-diols, as opposed to branched ones. Radiation scattering studies show a scattering pre-peak for the aqueous short linear diol mixtures,^{32,33} which do not seem to differ conclusively from aqueous–monol mixtures. There are quite a few computer simulation studies,^{34–37} which focus mostly on testing various force field issues and studying the short range structural properties. Gubskaya and Kusalik³⁵ report that, despite hydrogen bonding tendencies, little hydrophobic association is found through the study of direct space correlations. It is noteworthy that one of these studies reports calculations of the structure factors.

In the remainder of the paper, we first present the molecular models we have used as well as details of the protocol of our computer simulations. This is followed by an analysis of the simulation results. In the final section we analyse the adequacy of the concept of the Lifshitz state as well as the heuristic perspectives it opens up.

2 Theoretical and computational details

2.1 Theoretical considerations

One of the key properties of disordered liquid mixtures is homogeneity. This homogeneity is characterised by the fact that the total density $\rho = N/V$ and the species densities $\rho_i = N_i/V$ are scalar order parameters,³⁸ where $N = \sum_i N_i$ is the total number of particles, with N_i particles of each species i , and V is the total volume. In inhomogeneous systems, these quantities would be functions that depend on the spatial variables that characterise the inhomogeneity, such as the distance to a wall, for a confined liquid, or the orientation of the global order for a liquid crystal. Homogeneous order can nevertheless be further characterised by the measure of the fluctuations³⁸ $\delta\rho_i(\mathbf{r}) = \rho_i(\mathbf{r}) - \rho_i$ of the local densities $\rho_i(\mathbf{r})$ for each of the species at the spatial position \mathbf{r} . Such fluctuations can be measured through the pair correlation functions, defined as

$$g_{ij}(r) = \frac{\langle \rho_i(\mathbf{r}_1)\rho_j(\mathbf{r}_2) \rangle}{\rho_i\rho_j} \quad (1)$$

where the symbol $\langle \dots \rangle$ designates a statistical ensemble average, and $r = |\mathbf{r}_1 - \mathbf{r}_2|$. Similar quantities can be equally defined for various atom–atom correlations $g_{ab}(r)$ in the case of molecular mixtures,^{38,39} where a and b designate atoms belonging to molecular species. The atom–atom structure factors are defined as the Fourier transform

$$S_{ab}(k) = \delta_{ab} + \sqrt{\rho_a\rho_b} \int d\mathbf{r} [g_{ab}(r) - 1] \exp(i\mathbf{k} \cdot \mathbf{r}) \quad (2)$$

Both these functions are a direct measure of the fluctuations occurring in the liquid, and for all distances r and corresponding wave vectors k . For example, the peak structure in $g_{ab}(r)$ will designate the fluctuations corresponding to the presence of atomic cores of atoms a and b with periodicity $\sigma_{ab} \approx (\sigma_a + \sigma_b)/2$, where σ_a and σ_b designate the diameter of atoms a and b, respectively. The corresponding main peak in the structure factor $S_{ab}(k)$ will be positioned at $k \approx 2\pi/\sigma_{ab}$. Similarly, long range density or concentration fluctuations, such as those occurring at the approach of second order phase transitions, through the development of the Yukawa tail in the correlation function $g_{ab}(r) \rightarrow \exp(-r/\xi)/r$ when $r \rightarrow +\infty$, where ξ is the correlation length, lead to the appearance of an increase of the peak of $S_{ab}(k=0)$, through the well known relation to the particle number fluctuation³⁸

$$S_{ab}(k=0) = \frac{\langle N_a N_b \rangle - \langle N_a \rangle \langle N_b \rangle}{\sqrt{\langle N_a \rangle \langle N_b \rangle}} \quad (3)$$

The similarity of this expression to eqn (1) shows the common origin they have with fluctuations in general. These are very general textbook considerations.

However, clustering and micro-heterogeneity equally lead to specific long range domain–domain correlations, with a corresponding pre-peak in the structure factor $S_{ab}(r)$. We have shown several examples of such a pre-peak, in particular, for the correlations $S_{OO}(k)$ between the oxygen atoms of the hydroxyl groups in hydrogen bonding mixtures. Since these pre-peaks occur at a non-zero wave vector $k_p \approx 2\pi/d$, where d is the average domain size, one must not confuse micro-heterogeneity with the thermodynamic definition of concentration fluctuations as expressed through eqn (3). These latter can be measured through the Kirkwood–Buff integrals (KBIs),⁴⁰ which are defined as the integral of the correlation functions $g_{ab}(r)$ as:

$$G_{ab} = 4\pi \int_0^\infty dr r^2 [g_{ab}(r) - 1] \quad (4)$$

and are related to the $S_{ab}(k=0)$ through the expression

$$G_{ab} = \frac{S_{ab}(k=0) - \delta_{ab}}{\sqrt{\rho_a \rho_b}} \quad (5)$$

which shows clearly that they are a measure of thermodynamic fluctuations. Therefore, micro-heterogeneity, which concerns the pre-peak of $S_{ab}(k \neq 0)$ should not be confused with the Kirkwood–Buff integrals, which concern $S_{ab}(k=0)$. These latter quantities have been subject to various confusions in the previous literature, in particular with the concept of local solvation, which tend to indicate that connection between fluctuations and the local structure of complex liquids deserves further developments and clarifications.¹⁰

The KBIs can be related to thermodynamic quantities,⁴⁰ such as the partial molar volumes, the volume and the mole fraction derivatives of the chemical potentials through the expressions⁴¹

$$G_{ij} = (1 - \delta_{ij}) \left[\kappa_T^* - \frac{\bar{V}_i \bar{V}_j}{VD} \right] + \delta_{ij} \left[G_{12} + \frac{1}{x_i} \left(\frac{\bar{V}_j}{D} - V \right) \right] \quad (6)$$

where κ_T^* is the isothermal compressibility (in reduced units, which we often neglect since it is small for dense incompressible liquids), \bar{V}_m is the partial molar volume for species m , V is the total volume (which we approximate through the linear relation $V = (1-x)\bar{V}_1 + x\bar{V}_2$) and $D = D(x)$ is given by⁴¹

$$D(x) = -(1-x) \frac{\partial \beta \mu_1}{\partial x} = x \frac{\partial \beta \mu_2}{\partial x} \quad (7)$$

where μ_2 is the chemical potential of the diol species 2 in our convention ($\beta = 1/k_B T$ is the Boltzmann factor, k_B the Boltzmann constant and T the temperature).

This preliminary introduction to the rich nature of fluctuations in a mixture is needed to better appreciate the absence of it in the particular cases we propose to examine below.

2.2 Models and simulations

We study aqueous mixtures of ethanediol and 1,3-propanediol, as well as the ethanol mixture of the two same diols. For each type of binary mixture we have studied 3 diol mole fractions of $x = 0.2, 0.5$ and 0.8 , in addition to the respective pure liquids, $x = 0$ and $x = 1$, which we have studied independently previously.^{22,42,43} We have used the SPC/E model for water,⁴⁴ the TraPPE model for ethanol⁴⁵ and the two diols.⁴⁶ System sizes of $N = 2048$ and $N = 16\,000$ particles have been studied, the larger system in order to clarify the nature of the long range correlations in these systems, which is an important problem in these mixtures, as we shall discuss below. The initial configurations were generated by random molecular positioning, with the program PACKMOL.⁴⁷ The GROMACS code⁴⁸ was used for the molecular dynamics simulations, as in many of our previous works. Initial configurations were first energy minimized, then simulated in the constant NVT ensemble for a few hundred picoseconds. Then, 1–2 ns constant NPT runs were performed to stabilise the system under ambient conditions, with $T = 300$ K. Temperature was maintained constant using the Nosé–Hoover thermostat,^{49,50} and pressure was maintained at 1 atm using the Parrinello–Rahman barostat,^{51,52} with a time constant of 1 ps. Production runs were performed under the ambient conditions, for 2–10 ns, depending on systems and convergence of the long range tail of the atom–atom correlation functions, which is a particularly difficult issue in these mixtures.

By the definition of eqn (1), the atom–atom correlation functions should have a horizontal asymptote at very large separation. This asymptote is 1 in the thermodynamic limit $N \rightarrow \infty$ and $V \rightarrow \infty$. In finite size systems, however, this is never achieved, as demonstrated by Lebowitz and Percus⁵³ and the asymptote is $1 - \varepsilon/N$, where ε is related to the concentration fluctuations.^{53,54} In many cases, particularly for pure systems, this shift in the ideal asymptote is visible, and can be corrected by empirical methods of shifting, which we have demonstrated in previous works.⁵⁵ When domain–domain long range oscillations exist, they tend to mask the asymptote and this is a problem to determine the true value of the shift. In the case of the diol mixtures we studied, we found that the asymptotes were always void of domain oscillations, but it was difficult to obtain flat asymptotes. This will be illustrated below. In some

cases, we found it necessary to perform large scale and lengthy simulations to get better behaviour of the asymptote. We believe that this problem is inherent to this type of system, with sluggish equilibration and statistics, due to the fact that the hydroxyl groups of the diols are tied by the alkyl chains. The only cure seems to be to perform very long runs.

3 Results

In our previous computer simulation study of pure *n*-diols,²² we found that these types of alcohols, with the two hydroxyl groups constrained by a linking alkyl chain, produced a chain-like clustering similar to that found in mono-ols,^{56–58} as well as the corresponding pre-peak in the oxygen–oxygen structure factors, again similarly to mono-ols.⁵⁸ However, in contrast to the apparent pre-peak found in the experimental X-ray scattering of mono-ols,^{23–25} we observed only a weak shoulder in the calculated X-ray scattering intensities.²² The question which underlies this study is about how this dual property of these diols, namely the hydrogen bond induced microscopic order and the contrasting apparent disorder in the experimental observables, will affect the usual domain segregation patterns found in aqueous and alcohol mixtures of these *n*-diols.

3.1 Snapshots

We first illustrate through snapshots the striking and unexpected homogeneous randomness of these mixtures, for the case of equimolar mixtures and for the system size $N = 16\,000$ particles. Fig. 1 shows typical snapshots, with two colouring conventions. The upper row is for the water–ethanediol equimolar mixture. In Fig. 1a we show each of the species with different colors, which helps visualise species segregation. The snapshot shows that the species are somewhat segregated into small chain-like clusters,

but that the overall distribution is quite homogeneous. This is particularly striking in the case of water, because in all our previous works, we have always found that water tends to self-segregate into very large pockets,¹⁰ particularly well visible for equimolar mixtures. We attribute the present apparent homogeneity to the fact that each diol has two hydroxyl groups to bind with, which increases the water–diol hydrogen binding, but also reduces the water self-binding. Fig. 1b shows the same snapshot through the same angle, but the hydroxyl groups and the alkyl groups are colored differently. This permits us to observe that the mixing is dominated by the aggregation of the hydroxyl groups, but that this aggregation is quite random, similar to the randomisation of the alkyl groups. The lower row shows similar snapshots for ethanol–ethanediol mixtures. The visual observation of the small clustering and the apparent homogeneity of these systems explains many of the structural features which we discuss below for each of the mixtures studied.

3.2 Clusters

In order to confirm the visually homogeneous appearance observed in the snapshots of the previous section, we have calculated the cluster distribution of various atoms, and in particular the oxygens of the hydroxyl groups, which are responsible for the hydrogen bonding, which underlies the formation of clusters and segregated domains. From our previous cluster calculations, if the hydroxyl groups tend to preferentially self-bind in particular structures, such as chains or loops, then one should see a peak in the corresponding cluster distribution. For example, pure alcohols tend to form chain-like aggregates, which produce a peak in the cluster distribution.^{43,58} Pure diols also form chain-like clusters, which produce a cluster peak in the distribution,²² but it is weaker than in linear alkanols, which means there are fewer such clusters in diols than in mono-ols. Similarly, ethanol in benzene tends to form clustered domains, at the center of which the hydroxy groups form various loop-like clusters, which are equally detected through a peak in the cluster distribution.⁵⁹ This peak is absent in aqueous–alcohol mixtures, despite their strong micro-heterogeneity,¹⁰ because the alcohol molecules bind preferentially with water and consequently form fuzzy clusters⁵⁹ of all sizes.

Fig. 2a–d show the cluster distribution of the oxygen atoms inside each of the 4 mixtures (diol oxygen atoms in the main panel, and solvent oxygen atoms in the insets), and for 3 different concentrations. It is seen that all these curves show a decaying distribution, with no specific peaks. This does not mean that there are no chain clusters, but that such clusters are not dominating the distribution, as in the case of pure diols and mono-ols. These distributions are similar to those of the carbon atoms of the alkyl groups (not shown), the latter of which are supposed to obey random distribution since they are not hydrogen bound. This is a direct confirmation that there are few specific hydrogen bond based clusters. But, it does not exclude micro-heterogeneity, as seen in the case of aqueous–alcohol mixtures.⁵⁹ The clustering distribution of the oxygens of ethanediol presents a peculiarity that is not seen in longer diols: the presence of odd atom clusters is much less probable

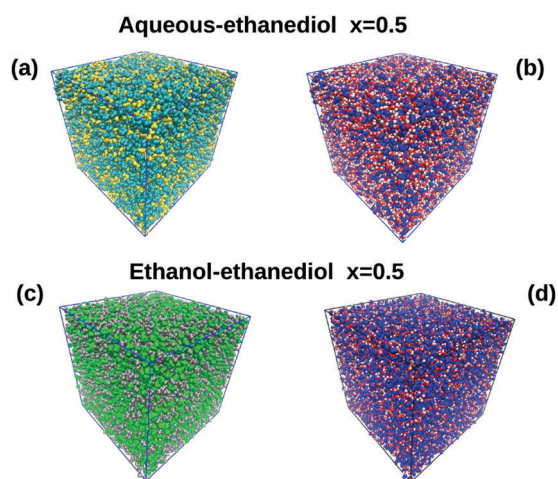


Fig. 1 Snapshots of the equimolar water–ethanediol (upper row) and ethanol–ethanediol (lower row) shown with 2 different colouring conventions. (a) Water molecules are shown in cyan and diol molecules in yellow; (b) oxygen atoms are in red, hydrogen in white and methylene groups in blue; (c) molecules are shown in gray and diol molecules in green; (d) the same colouring convention as in (b).

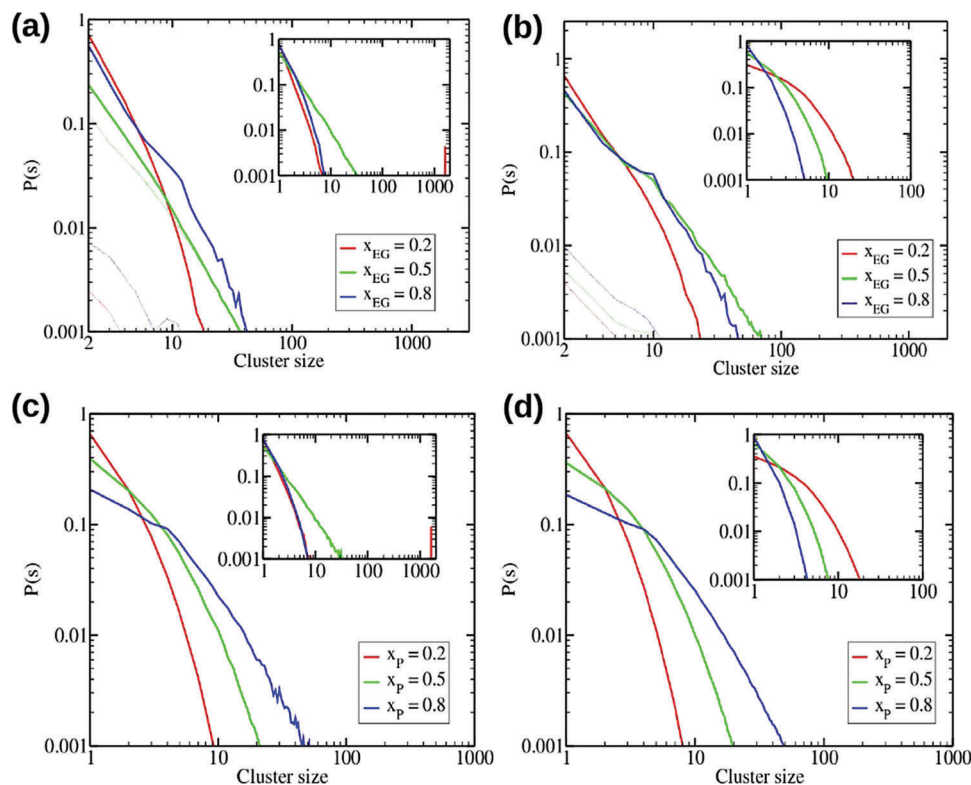


Fig. 2 Clusters distributions of the diol oxygen sites (main panels) and solvent oxygen sites (insets), versus the cluster size, for (a) the water–ethanediol mixtures, (b) the ethanol–ethanediol mixtures, (c) the water–propanediol mixtures and (d) the ethanol–propanediol mixtures. The diol concentrations are shown in red for $x = 0.2$, green for $x = 0.5$ and blue for $x = 0.8$. The thin dotted lines in (a) and (b) are explained in the text.

than the even ones. This asymmetry is illustrated by showing the odd atom distribution as thinner dotted lines in Fig. 2a and b. The short alkyl chain constraint imposes a form of hydrogen bonding since the end chain hydroxyl groups are strongly correlated with the nearing methylene groups. However, as we will see below, this constraint is not apparent in the correlation functions and the structure factors, because of the overall disorder of the hydrogen bonding.

3.3 Structure functions

In order to detect micro-heterogeneity, we need to look at the long range correlations between the oxygen atoms, and the associated pre-peak in the corresponding structure factors. In a previous paper,⁵⁹ we distinguished between the short range depletion in the correlation functions, past the first peak of $g_{ab}(r)$, which is a signature of linear chain-like clusters involving atoms a and b (usually the oxygen atoms in the case of hydrogen bonded systems), and the long range domain oscillations, which are a signature of micro-segregation. The first type of correlation is seen for example in neat alcohol or ionic liquids,^{10,60} while the second type is seen in micro-heterogeneous mixtures. These two types of clustering produce two distinct pre-peaks. The chain correlation produces a pre-peak usually in the $k_p \approx 1 \text{ \AA}^{-1}$ range, while the domain pre-peak is for the $0 < k_p < 1 \text{ \AA}^{-1}$ range.

Following this remark and what we have obtained so far for the present systems, we expect chain pre-peaks, but no domain pre-peaks.

3.3.1 Aqueous–ethanediol mixtures. Fig. 3a shows specific oxygen–oxygen correlations, and Fig. 3b the corresponding structure factors, for the three diol mole fractions we have studied. Pure liquid correlations are equally shown in black lines. It is generally seen that water oxygen–oxygen correlations are stronger than the corresponding diol correlations, and they behave in an opposite manner: for water, they become stronger with decreasing water content, while for the diol they decrease with decreasing diol content. This is a generic behaviour of aqueous mixtures, which we have reported previously in various contexts. It is a direct consequence of the higher charges on water model oxygen and hydrogen sites than on the hydroxyl groups of the diol solute model, which mimic hydrogen bonding through classical Coulomb interactions. At lower water content, water always prefers to self-bind to itself rather than to the dominating amount of surrounding solutes. It is seen that the long range correlations are rapidly screened, and hence there is no long range domain order.

Since the snapshots reveal small chain-like clusters, we expect to see these through a pre-peak in the oxygen–oxygen structure factors. Fig. 3b shows that such a pre-peak – or a plateau – exists for the diol and cross-structure factors (left and middle panels), but the water structure factor (right panel) shows a rather enhanced $k = 0$ peak. The absence of a clear cluster pre-peak for water is very intriguing. This is actually a capital point for the concept of the Lifshitz state. It seems that the water correlations “hesitate” between a cluster pre-peak

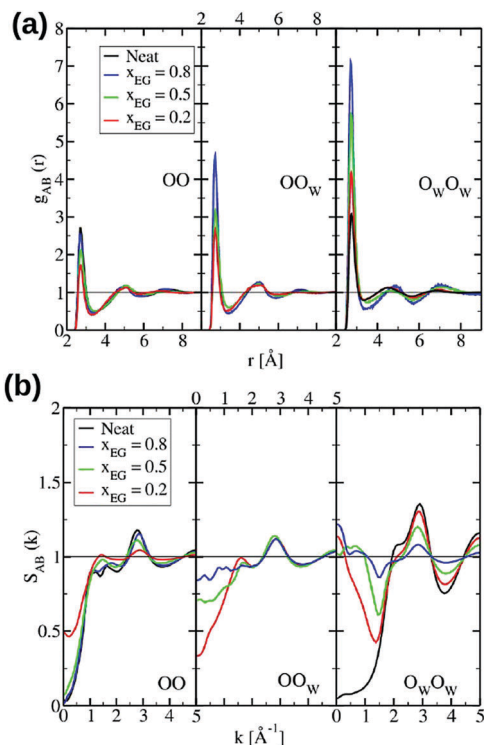


Fig. 3 Oxygen–oxygen correlation functions (a) and structure factors (b) for the aqueous–ethanediol mixtures. The diol concentrations are shown in blue for $x = 0.2$, green for $x = 0.5$ and red for $x = 0.8$. Pure solvent data are shown in black. The left panel for the oxygen atoms of the diol, the middle panel for the cross-correlations and the right panel for the oxygen atoms of water.

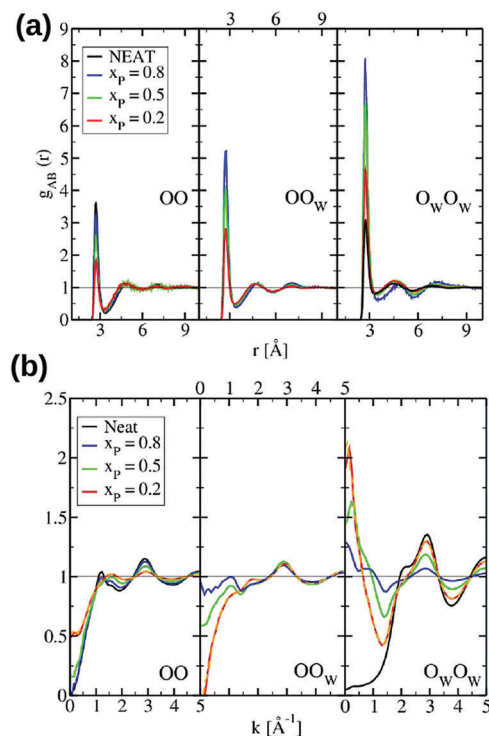


Fig. 4 Oxygen–oxygen correlation functions (a) and structure factors (b) for the aqueous–propanediol mixtures, with the same colouring conventions as in Fig. 3. The dashed yellow curve is for $N = 16000$ particles in the case of $x = 0.2$.

and a concentration fluctuation $k = 0$ peak. We will come back to this point later.

The increase of the $k = 0$ peak is coupled to the behaviour at larger k -values. For example, it is interesting to see that both the $k = 0$ and the cluster pre-peak of the oxygen correlations of the diol (left panel) increase when the diol content decreases (for $x = 0.2$), which is also accompanied by a decrease of the main peak at $k_M \approx 2.7 \text{ \AA}^{-1}$. A similar effect is also observed for the water oxygen correlations.

3.3.2 Aqueous–propanediol mixtures. Fig. 4a and b show the same quantities as in Fig. 3a and b, but for aqueous–propanediol mixtures. The overall behaviour of the correlations is very similar to that observed in Fig. 3a and b. We see that the real space correlations show a higher first peak for aqueous–propanediol than for aqueous–ethanediol. Since the charges on the oxygen atoms are the same between the 2 models, the increase in the oxygen correlations comes from the presence of an additional methylene group for the propanediol. The cluster pre-peak in the structure factor for the oxygen atoms of the propanediol is better defined than for ethanediol, which was also the case for the pure diol.²² This is probably another indirect effect of the additional methylene groups, which enforce oxygen atom correlations through hydrophobic effects. We again observe that the water oxygen atom structure factors show no sign of any clear pre-peak, and rather a $k = 0$ increase.

For the case of $x = 0.2$, we have shown a comparison with the $N = 16000$ particles (yellow dashed curve), where the domain pre-peak type feature vanishes for the larger system, indicating that such a feature is a numerical artifact.

3.3.3 Ethanol–ethanediol mixtures. The oxygen–oxygen correlations and structure factors of the ethanol–ethanediol mixtures are shown in Fig. 5a and b. Looking at $g_{ab}(r)$, we see that the diol behaves like water: the main peak increases with decreasing concentrations of the diol, while it is the opposite for ethanol. This is very different than what we have observed so far when mixing alcohols with non-associated solutes: the alcohol always behaved like water, since the alcohol molecules would always prefer to hydrogen bond with each other, in the middle of non-bonding solutes. The fact that now the diol behaves like water in the presence of ethanol is directly imputable to the alkyl constraint linking the two hydroxyl groups. In fact, this is consistent with water, since one could view water as a “zero-level diol” (with a zero alkyl chain).

Since both pure liquids have a pre-peak,²² we expect to see in Fig. 5b pre-peaks corresponding to $k_p \approx 1 \text{ \AA}^{-1}$, which is indeed the case. But we also see smaller pre-peaks for smaller k -values. These cannot be compared to the domain pre-peaks, which are always very high, with a magnitude ranging from 5 to 50,¹⁰ while those we see here are about 1. Indeed, there is no corresponding medium-to-long-range correlations in Fig. 5a. We believe that these small pre-peaks are artifacts of the Fourier transforms, coming from small irregularities in the flat

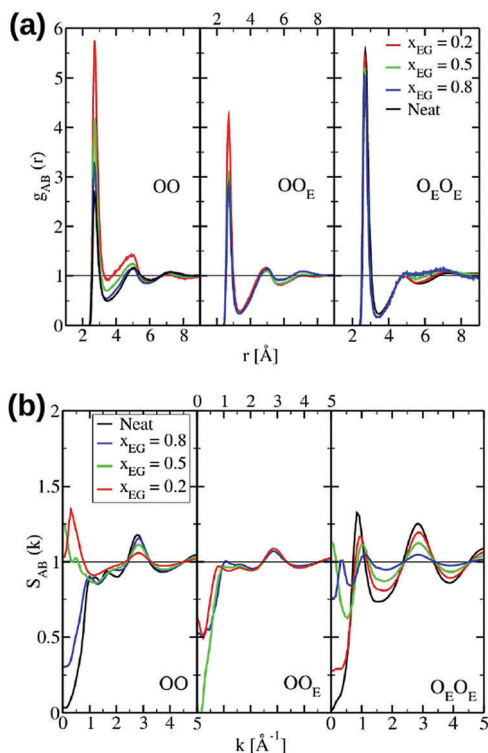


Fig. 5 Oxygen–oxygen correlation functions (a) and structure factors (b) for the ethanol–ethanediol mixtures, with the same colouring conventions as in Fig. 3.

asymptotic region of $g_{ab}(r)$, which are due to slow statistical convergence of these particular systems, which we have mentioned in Section 2.2.

3.3.4 Ethanol–propanediol mixtures. Fig. 6a and b show the same quantities as shown in Fig. 5a and b, but for ethanol–propanediol mixtures. We again observe in Fig. 6a that the diol correlations behave like water, but with a smaller magnitude. This is probably due to the fact that the alkyl tail linking the two hydroxyl groups of propanediol is longer. The shorter this link, the closer the behaviour with water expected.

The structure factors in Fig. 6b bear a close resemblance with Fig. 5b. We note again a small pre-peak for small k -values, which again comes from statistical problems in the asymptotes of $g_{ab}(r)$. In the case of $x = 0.2$, the $N = 16\,000$ data (yellow dashed curve) show that this artifact tends to disappear.

3.3.5 Methyl group correlations. In Fig. 7 we show some correlations of the chosen methyl group correlations, mostly to see the important differences with that of the oxygen atoms, the latter of which dominate the correlations in these liquids. For $g_{MM}(r)$, we note the smaller amplitude of the first peaks, as compared with those of hydrogen bonding sites, as well as the weaker variation with the mole fraction. For the structure factors, we essentially note that they look much like those of ordinary Lennard-Jones mixtures. Both observations point to the fact that the methyl groups look essentially weakly interacting and correlating, although they play an essential role in the randomisation and homogeneity of the hydroxyl groups. They point to the extreme asymmetric role of hydrophilic and

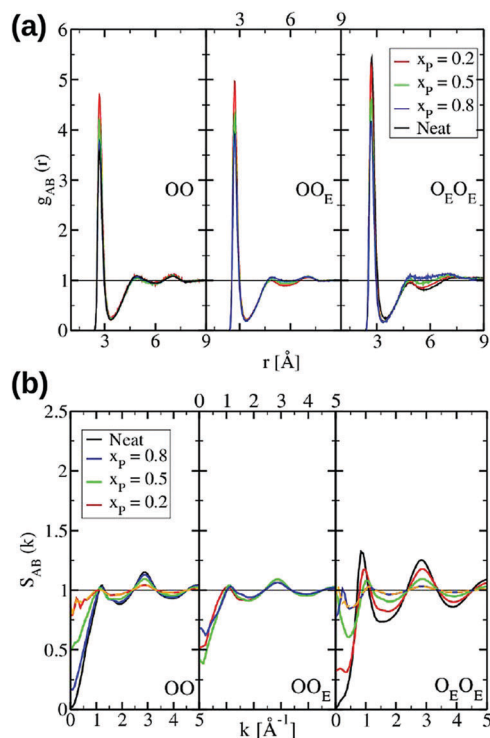


Fig. 6 Oxygen–oxygen correlation functions (a) and structure factors (b) for the ethanol–propanediol mixtures, with the same colouring conventions as in Fig. 3. The dashed yellow curve is for $N = 16\,000$ particles in the case of $x = 0.2$.

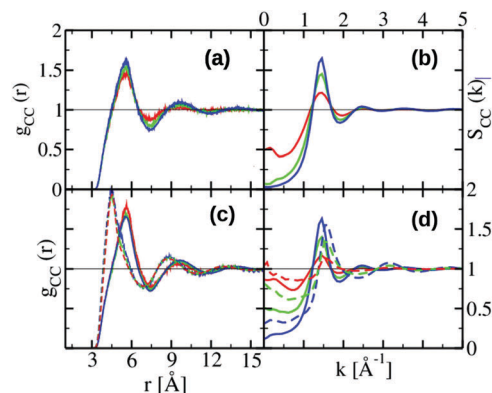


Fig. 7 Central methylene group correlations (a and c) and structure factors (b and d) for the aqueous–propanediol (upper row a and b) and ethanol–propanediol (lower row c and d). The line colors correspond to different concentrations, with the same convention as Fig. 3. Full lines for the methylene of ethanediol and dashed for that of ethanol.

hydrophobic moieties, although both are needed to explain the complexity of such mixtures.

3.4 Kirkwood–Buff integrals

Kirkwood–Buff integrals are evaluated through eqn (4), where, in practice, the upper bound is limited to half the box size $l_B = L_{\text{box}}/2$. The validity of this calculation requires therefore that the correlation functions have decayed to 1 before the inter-site distance l_B is reached. For a system exhibiting a

micro-structure, the long range part of the correlation is affected by it, hence larger boxes are required. This problem adds to the inherent LP correction mentioned in Section 2.2. We refer to the next subsection for some of the numerical problems met in calculating the KBIs of the present mixtures.

Fig. 8 shows the Kirkwood–Buff integrals of each of the 4 mixtures studied in the previous sections. It is seen that the KBIs of the aqueous mixtures, shown in Fig. 8a and c, are near ideal, and are in good agreement with the experimental data in the case of the aqueous–ethanediol system,³¹ the only such data we could find in the literature. We note that Geerke and van Gusteren³⁷ have previously reported the KBIs for aqueous ethylene glycol, in the small concentration regime, and also in good agreement with the experimental data of Marcus.³¹ The ideal KBIs, corresponding to the choice $D(x) = 1$ in eqn (6), are plotted as full lines. This ideality is an indication that these mixtures have low concentration fluctuations, in addition to being very homogeneous. There is more uncertainty in the data for water than the diol and cross KBIs. This is a direct consequence of the sluggishness of the dynamics and the statistics.

In contrast, the ethanol–diol mixtures show somewhat weak non-ideality. The ideal KBIs with $D(x) = 1$ are plotted as dashed lines. First of all, because of the proximity of the volumes of ethanol and the diols, all the ideal KBIs are grouped quite close to each other, as can be seen from eqn (6). In the case of ethanol–ethanediol, we have calculated more points, using 4 ns and 8 ns statistics for the $N = 2048$ systems. In order to match the simulated KBIs, we have extracted the $D(x)$ function from these simulated points, by inverting eqn (6), following a recipe explained in ref. 59. The KBIs were then re-evaluated by using this $D(x)$ and are shown in full lines in Fig. 8b and d. The functions $D(x)$ are plotted in the respective insets and show small deviations from $D(x) = 1$, the latter of which is the ideal value corresponding to ideal chemical potentials $\beta\mu_i = \ln(\rho_i)$. This is the principal reason why we claim that these KBIs are nearly ideal. For example, in the case of aqueous–alcohol mixtures, which are very micro-heterogeneous, the maximum of the water–water KBIs often ranges in 500–10 000.⁴¹ The observed near ideality of the KBIs indicates that there are very few concentration fluctuations in these mixtures. This is consistent with the visual homogeneity observed in the snapshots.

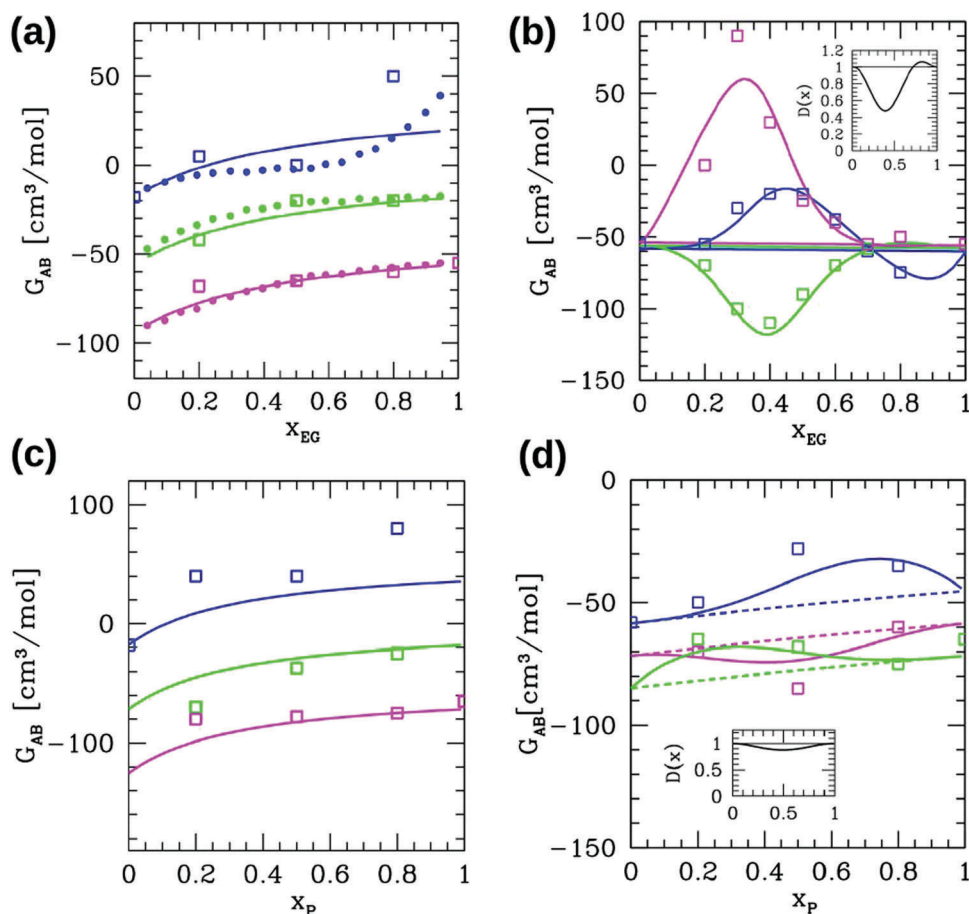


Fig. 8 Kirkwood–Buff integrals, versus the diol mole fractions, of the aqueous–ethanediol mixtures (a), ethanol–ethanediol mixtures (b), aqueous propanediol mixtures (c) and ethanol–propanediol mixtures (d). Blue line is for solvent–solvent, green for solvent–diol and magenta for diol–diol KBI. The squares represent the simulation results, the full or dashed lines correspond to different choices of $D(x)$, shown in the inset for the ethanol–diol mixtures (see the text). The dots in (a) are experimental results from ref. 31.

The fact that aqueous–diol mixtures are more ideal than ethanol–diol mixtures is very non-intuitive, and turns out to be a key feature of these mixtures. Indeed, one would expect that the presence of methyl groups in ethanol would help randomise these mixtures much more than in the case of water. Our explanation for this contradicting finding is that the ideality of these aqueous mixtures is only apparent, and that it is the result of a competition between the self-aggregation tendency of water, as observed in all other types of mixtures, and the constraint imposed on the diol hydroxyl groups by the linking the alkyl chain. In other words, there is a very strong hidden order in the aqueous diol mixtures, which produces an apparent ideality and decrease of concentration fluctuations, without domain segregation. Conversely, the alkyl groups of the ethanol molecules hinder this hidden ordering, which would be there only if the hydroxyl groups were present. This hinderance produces an apparent fluctuation and non-ideality, which is seen in the KBIs, but also in the sluggishness of the dynamics of these ethanol–diol mixtures.

3.5 Influence of system size and statistics

As mentioned previously, these diol mixtures are very sluggish, hence long statistics are required, despite the fact that these systems look homogeneous. We discuss here the problems of obtaining the KBIs from numerical integration of the correlation functions in finite size simulations.

Fig. 9 shows the effects of the system size and statistics on the correlation functions, as illustrated for the case of oxygen–oxygen correlations of the aqueous–propanediol mixture for 20% diol. 2 system sizes are reported $N_1 = 2048$ and $N_2 = 16\,000$. For system size N_1 , we have accumulated statistics for 1 ns (golden curve) and 8 ns (blue curve). For the system size N_2 , we have accumulated statistics for 0.5 ns (red curve) and 4 ns (green curve). The main panel shows that, for atomic distances below 10 Å, all statistics are indistinguishable. However, the inset demonstrates the deviations in the long range parts. It is clear that the longer the runs, the better the asymptotes stabilize closer to 1. The data shown are unshifted for the LP correction mentioned in Section 2.2. Panel (b) shows the corresponding “running” Kirkwood–Buff integral, defined as:

$$G_{ab}(r) = 4\pi \int_0^r ds s^2 [g_{ab}(s) - 1] \quad (8)$$

This integral should asymptotically reach the value of the correct KBI (namely about $G_{O_wO_w} \approx 42 \text{ cm}^3 \text{ mol}^{-1}$, as reported in Fig. 8a). This figure shows the dramatic differences one expects from poor statistics. All the tails have been corrected for the proper asymptote shift to bring them to the expected value of 1 (which is why they are almost horizontal). The deviation is not apparent until $r \approx 10 \text{ Å}$ for most of the data. It is clear that the small N_1 system is nearly appropriate, provided long statistics (8 ns) are performed. Even then, one sees that the asymptote is not quite flat. Short runs for the larger system size produce artificial oscillations (red curves), which disappear with 4 ns statistics (green curve), and converge to an acceptable asymptote, which permits the extraction of the KBI value

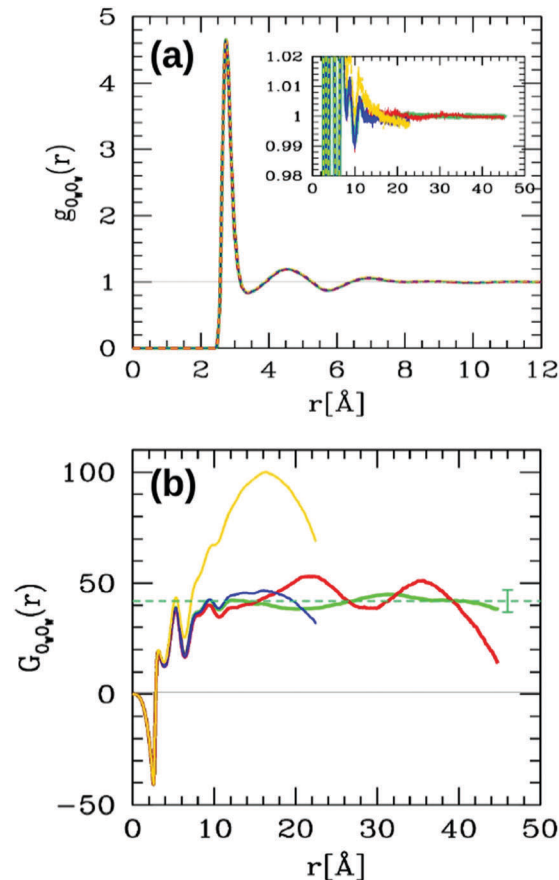


Fig. 9 Influence of system size and statistics. (a) Main panel: water oxygen–oxygen correlations $g_{O_wO_w}(r)$ for 20% propanediol in water; inset: zoom on the tail (uncorrected). (b) Running KBIs. Gold line is for $N_1 = 2048$ and 1 ns, blue for N_1 and 8 ns, red line for $N_2 = 16\,000$ and 0.5 ns, green line for N_2 and 4 ns (some lines are dashed for better visibility). The horizontal dashed line is the final retained value for KBI, with indicative error bar.

reported in Fig. 8a. The dashed green line drawn through the tail of the RKBI indicates our estimate of the KBIs, together with the error bar, which is about $10 \text{ cm}^3 \text{ mol}^{-1}$. The resulting KBI value is above the experimental value, but this could well be a model problem, which is an expected drawback. But the correct trend of the KBIs, namely the quasi-ideality of this system, as seen in Fig. 8a, has been accurately reproduced by the models and simulations. Longer statistics result in somewhat reduced tail oscillations in the KBIs, but only systems larger than N_2 would lead to more precise values. However, we believe that the present estimate, as shown in Fig. 8, demonstrates the correct overall behaviour. Other methodologies than eqn (8), such as that proposed in ref. 61, which takes into account the scaling of fluctuations with the system size for the case of moderate heterogeneity, could be adapted to the Lifshitz phase disorder, precisely because of the reduced heterogeneity.

3.6 Thermodynamics

In addition to the structural properties, it is useful to test the validity of the force field models by comparing with thermodynamic data such as the total density and the enthalpy.

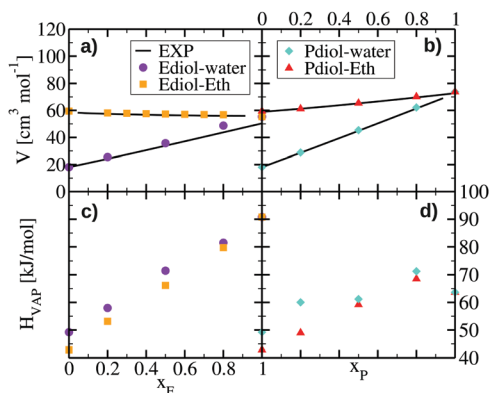


Fig. 10 Thermodynamic properties. Volumes in (a and b), enthalpies in (c and d). Black line for experimental data,^{62–65} purple circles for aqueous–ethanediol, gold squares for ethanol–ethanediol, cyan symbols for aqueous–propanediol and red triangles for ethanol–propanediol.

In Fig. 10 we show the general trends for the molar volumes and enthalpies of the simulated systems, and compare with experiments in the case of the volumes, which are found to be in excellent agreement in all cases. As for the enthalpies, we note that both water and ethanol mixtures of a given diol are quite close to each other. We also note that the enthalpies of pure diols are more negative than those of these two solvents, because of the presence of the 2 hydroxyl groups, which clearly dominate the energetic parts. One can argue that the sampling problems we find in these mixtures are equally due to the fact that the large negative energies contribute to locking of the local equilibrium and hinder the statistical refreshment of the configurations, enforcing lengthy statistics.

4 Discussion and conclusion

The principal feature that emerges from our study is the essential role played by the constraint of the alkyl chain between the two hydroxyl groups of these 1,*n*-diols. These double hydroxyl groups help randomize the water and alcohol solvents, but the presence of the alkyl constraint produces a hidden order, which is not detected by the cluster and correlation function analysis. We infer this hidden order from the curious absence of self-segregation of water, as seen in all other types of solutes, as well as the apparent ideality of the KBIs of these aqueous mixtures. When comparing these features with the findings of the ethanol–diol mixtures, we see that the alkyl tails of the alcohol bring a disturbance in this hidden order, responsible for the weak non-ideality seen in the KBIs. In all of the previously investigated mixtures with hydrogen bonding species, the predominant feature was the appearance of a segregated domain pre-peak in the atom–atom structure factors. The present mixtures, despite hydrogen bonding tendencies, do not possess this pre-peak. The presence of hydrogen bonding interactions imposes a specific binding, but this bonding does not produce sufficient local order to induce a pre-peak. Yet, this is not random disorder. In other

words, the absence of a pre-peak does not necessarily imply random disorder.

This hidden order is the reason why we propose considering these mixtures as a new type of disorder. Due to the absence of domain–domain correlations, and the appealing similarity to the disappearance of the pre-peak in the micro-emulsion when approaching the Lifshitz point from the side of the layer ordered phase, we propose to call this new type of disorder the Lifshitz state. As hinted in the Introduction, through this naming, we propose a unification scheme for molecular and micro-emulsions. Although micro-emulsions are micro-heterogeneous at a larger spatial degree, with larger water and oil domains, they share the same microscopic hydrogen bonding interaction and hydrophobic/hydrophilic competition patterns. Similarly, even though molecular emulsions cannot manifest the same macroscopic ordered phase transitions as micro-emulsions, they both certainly share similarities in the pre-transitional fluctuations, because of the same microscopic origins, such as the hydrophobic interactions, for example. The present study hints at the richness of the underlying disorder, from the molecular emulsion side.

Whereas the Lifshitz point in micro-emulsions can be reached by moving through the phase diagram, the present Lifshitz state is a permanent physical state. It can be “reached” by changing the nature of the solute particle, by breaking the alkyl chain or branching the diol, in which case the resulting mixture would show the same molecular emulsion pre-peak as water–methanol or water–ethanol. This is a fictitious operation for the present case, but in the case of chemically induced bonding, this passage from a molecular emulsion to a Lifshitz state could well occur. Such a situation is likely to occur in biomaterial liquids, which have a rich internal kinetics. The concept of Lifshitz state or disorder could be useful in such contexts.

The type of special disorder found in these mixtures has suggestive analogies to that in the separation of water from a simple disordered Lennard-Jones fluid.⁴² Both liquids are disordered, but the disorder in water has a richness, which reveals itself under mixing with other liquids. Micro-heterogeneity is one such property, which is not found in the mixtures of simple liquids, such as the mixture of alkanes, for example.⁵⁴ Through this paper, we have introduced a new type of structured disorder, which is different from micro-heterogeneity and clustering, but which is not a strict random disorder either, and which we call the Lifshitz disorder.

There is a rich variety in the ordered phases, whether these are crystalline or liquid crystalline phases. The richness of these orders is witnessed through the macroscopic order parameter, which is often the 1-body density $\rho^{(1)}(1)$, where argument indicates that this is a function of spatial and/or orientational degree of freedom of each molecule. This 1-body function can be formally related to a spontaneous macroscopic field through modern density functional theory, and this field orders the whole system. In contrast, the order parameter of a disordered liquid is the scalar density ρ , which is therefore unable to express the underlying richness of the disorder. Indeed, the

order of the macroscopically disordered phase is local. But the local density $\rho(1)$ is a random variable, whose statistical average wipes out all the interesting richness to give a scalar: $\langle \rho(1) \rangle = \rho$. However, pair correlation functions $\rho^{(2)}(1,2) = \langle \rho(1)\rho(2) \rangle$, which are in fact a measure of fluctuations, allow us to measure this disorder at small molecular separation, or in the small wave vector limit, as we have seen through this study. The measure of the richness of disorder is important in the case of soft matter and bio-matter, which are essentially disordered systems, but with a rich microscopic order. We hope that the concept of Lifshitz state is a first step in classifying the forms of disorder, and that it will be helpful in future studies.

Acknowledgements

This work has been partially supported by the Croatian Science Foundation under project 4514, "Multi-scale description of meso-scale domain formation and destruction". M. Požar thanks the French Embassy in Croatia for financial support through "bourse du Gouvernement Français".

References

- 1 R. M. Hornreich, M. Luban and S. Shtrikman, Critical behavior at the onset of k -space instability on the λ line, *Phys. Rev. Lett.*, 1975, **35**, 1678–1681.
- 2 S.-H. Chen, S.-L. Chang and R. Strey, Structural evolution within the one-phase region of a three-component microemulsion system: water-*n*-decane-sodium-bis-ethylhexylsulfosuccinate (aot), *J. Chem. Phys.*, 1990, **93**(3), 1907–1918.
- 3 A. Ciach and W. T. Gozdz, 7 nonelectrolyte solutions exhibiting structure on the nanoscale, *Annu. Rep. Prog. Chem., Sect. C: Phys. Chem.*, 2001, **97**, 269–314.
- 4 R. Hołyst and B. Przybylski, Topological lifshitz line, off-specular scattering, and mesoporous materials, *Phys. Rev. Lett.*, 2000, **85**, 130–133.
- 5 G. Gompper and M. Schick, Lattice model of microemulsions, *Phys. Rev. B: Condens. Matter Mater. Phys.*, 1990, **41**, 9148–9162.
- 6 G. Gompper, R. Hołyst and M. Schick, Interfacial properties of amphiphilic systems: the approach to lifshitz points, *Phys. Rev. A: At., Mol., Opt. Phys.*, 1991, **43**, 3157–3160.
- 7 S. Komura, Mesoscale structures in microemulsions, *J. Phys.: Condens. Matter*, 2007, **19**(46), 463101.
- 8 D. Frenkel, Structure of hard-core models for liquid crystals, *J. Phys. Chem.*, 1988, **92**(11), 3280–3284.
- 9 R. D. Koehler, K.-V. Schubert, R. Strey and E. W. Kaler, The lifshitz line in binary systems: structures in water/c4e1 mixtures, *J. Chem. Phys.*, 1994, **101**(12), 10843–10849.
- 10 A. Perera, From solutions to molecular emulsions, *Pure Appl. Chem.*, 2016, **88**(3), 189–206.
- 11 S. Dixit, J. Crain, W. C. K. Poon, J. L. Finney and A. K. Soper, Molecular segregation observed in a concentrated alcohol-water solution, *Nature*, 2002, **416**, 829–832.
- 12 S. K. Allison, J. P. Fox, R. Hargreaves and S. P. Bates, Clustering, microimmiscibility in alcohol-water mixtures: evidence from molecular-dynamics simulations, *Phys. Rev. B: Condens. Matter Mater. Phys.*, 2005, **71**, 024201.
- 13 D. Subramanian, D. A. Ivanov, I. K. Yudin, M. A. Anisimov and J. V. Sengers, Mesoscale inhomogeneities in aqueous solutions of 3-methylpyridine and tertiary butyl alcohol, *J. Chem. Eng. Data*, 2011, **56**(4), 1238–1248.
- 14 E. A. Ploetz and P. E. Smith, A kirkwood-buff force field for the aromatic amino acids, *Phys. Chem. Chem. Phys.*, 2011, **13**, 18154–18167.
- 15 E. A. Ploetz, N. Benteitis and P. E. Smith, Kirkwood-buff integrals for ideal solutions, *J. Chem. Phys.*, 2010, **132**(16), 164501.
- 16 C. S. Santos, H. V. R. Annapureddy, N. S. Murthy, H. K. Kashyap, E. W. Castner Jr. and C. J. Margulis, Temperature-dependent structure of methyltributylammonium bis-(trifluoromethylsulfonyl)amide: X-ray scattering and simulations, *J. Chem. Phys.*, 2011, **134**(6), 064501.
- 17 A. Triolo, O. Russina, B. Fazio, R. Triolo and E. Di Cola, Morphology of 1-alkyl-3-methylimidazolium hexafluorophosphate room temperature ionic liquids, *Chem. Phys. Lett.*, 2008, **457**(4–6), 362–365.
- 18 H. K. Kashyap, J. J. Hettige, H. V. R. Annapureddy and C. J. Margulis, Saxs anti-peaks reveal the length-scales of dual positive-negative and polar-apolar ordering in room-temperature ionic liquids, *Chem. Commun.*, 2012, **48**, 5103–5105.
- 19 A. A. H. Pádua, M. F. Costa Gomes and J. N. A. Canongia Lopes, Molecular solutes in ionic liquids: a structural perspective, *Acc. Chem. Res.*, 2007, **40**(11), 1087–1096, PMID: 17661440.
- 20 B. Kežić and A. Perera, Aqueous *tert*-butanol mixtures: a model for molecular-emulsions, *J. Chem. Phys.*, 2012, **137**(1), 014501.
- 21 M. Teubner and R. Strey, Origin of the scattering peak in microemulsions, *J. Chem. Phys.*, 1987, **87**(5), 3195–3200.
- 22 M. Požar and A. Perera, On the existence of a scattering pre-peak in the mono-ols and diols, *Chem. Phys. Lett.*, 2017, **671**, 37–43.
- 23 A. H. Narten and A. Habenschuss, Hydrogen bonding in liquid methanol and ethanol determined by X-ray diffraction, *J. Chem. Phys.*, 1984, **80**(7), 3387–3391.
- 24 S. Sarkar and R. N. Joarder, Molecular clusters and correlations in liquid methanol at room temperature, *J. Chem. Phys.*, 1993, **99**(3), 2032–2039.
- 25 M. Tomšič, A. Jamnik, G. Fritz-Popovski, O. Glatter and L. Vlček, Structural properties of pure simple alcohols from ethanol, propanol, butanol, pentanol, to hexanol: comparing monte carlo simulations with experimental saxs data, *J. Phys. Chem. B*, 2007, **111**(7), 1738–1751.
- 26 J.-Y. Huot, E. Battistel, R. Lumry, G. Villeneuve, A. Lavallee, J.-F. Anusiem and C. Jolicoeur, A comprehensive thermodynamic investigation of water-ethylene glycol mixtures at 5, 25, and 45 °C, *J. Solution Chem.*, 1988, **17**(7), 601–636.
- 27 G. Douheret, A. Pal, H. Høiland, O. Anowi and M. I. Davis, Thermodynamic properties of (ethan-1,2-diol + water) at the

- temperature 298.15 K. i. molar volumes, isobaric molar heat capacities, ultrasonic speeds, and isentropic functions, *J. Chem. Thermodyn. Thermochem.*, 1991, **23**(6), 569–580.
- 28 G. Ternström, A. Sjöstrand, G. Aly and Å. Jernqvist, Mutual diffusion coefficients of water + ethylene glycol and water + glycerol mixtures, *J. Chem. Eng. Data*, 1996, **41**(4), 876–879.
- 29 S. D. Deosarkar and A. S. Ghatbandhe, Molecular interactions and structures in ethylene glycol–ethanol and ethylene glycol–water solutions at 303 K on densities, viscosities, and refractive indices data, *Russ. J. Phys. Chem. A*, 2014, **88**(1), 32–36.
- 30 S. Azizian and M. Hemmati, Surface tension of binary mixtures of ethanol + ethylene glycol from 20 to 50, *J. Chem. Eng. Data*, 2003, **48**(3), 662–663.
- 31 Y. Marcus, Preferential solvation in mixed solvents. 12. aqueous glycols, *J. Mol. Liq.*, 2003, **107**(1), 109–126.
- 32 H. Abdelmoulaoui, H. Ghalla, S. Nasr, M. Bahri and M.-C. Bellissent-Funel, Hydrogen-bond network in liquid ethylene glycol as studied by neutron scattering and {DFT} calculations, *J. Mol. Liq.*, 2016, **220**, 527–539.
- 33 T. Takamuku, Y. Tsutsumi, M. Matsugami and T. Yamaguchi, Thermal properties and mixing state of diol–water mixtures studied by calorimetry, large-angle X-ray scattering, and nmr relaxation, *J. Phys. Chem. B*, 2008, **112**(42), 13300–13309, PMID: 18826183.
- 34 L. Saiz, J. A. Padro and E. Guardia, Structure of liquid ethylene glycol: a molecular dynamics simulation study with different force fields, *J. Chem. Phys.*, 2001, **114**(7), 3187–3199.
- 35 A. V. Gubskaya and P. G. Kusalik, Molecular dynamics simulation study of ethylene glycol, ethylenediamine, and 2-aminoethanol. 2. Structure in aqueous solutions, *J. Phys. Chem. A*, 2004, **108**, 7165–7178.
- 36 O. V. de Oliveira and L. C. G. Freitas, Molecular dynamics simulation of liquid ethylene glycol and its aqueous solution, *THEOCHEM*, 2005, **728**(1–2), 179–187.
- 37 D. P. Geerke and W. F. van Gunsteren, The performance of non-polarizable and polarizable force-field parameter sets for ethylene glycol in molecular dynamics simulations of the pure liquid and its aqueous mixtures, *Mol. Phys.*, 2007, **105**(13–14), 1861–1881.
- 38 J.-P. Hansen and I. R. McDonald, *Theory of Simple Liquids*, Academic Press, Elsevier, Amsterdam, 3rd edn, 2006.
- 39 C. G. Gray and K. E. Gubbins, *Theory of Molecular Fluids. Volume I: Fundamentals, volume 1 of International Series of Monographs on Chemistry (Book 9)*, Oxford University Press, 1st edn, 1985.
- 40 J. G. Kirkwood and F. P. Buff, The statistical mechanical theory of solutions. i, *J. Chem. Phys.*, 1951, **19**(6), 774.
- 41 E. Matteoli and L. Lepori, Solute-solute interactions in water. ii. An analysis through the kirkwood-buff integrals for 14 organic solutes, *J. Chem. Phys.*, 1984, **80**(6), 2856.
- 42 A. Perera, On the microscopic structure of liquid water, *Mol. Phys.*, 2011, **109**(20), 2433–2441.
- 43 M. Mijaković, B. Kežić, L. Zoranić, F. Sokolić, A. Asenbaum, C. Pruner, E. Wilhelm and A. Perera, Ethanol–water mixtures: ultrasonics, brillouin scattering and molecular dynamics, *J. Mol. Liq.*, 2011, **164**(1–2), 66–73.
- 44 H. J. C. Berendsen, J. P. M. Postma, W. F. van Gunsteren and J. Hermans, *Intermol. Forces*, Chapter Interaction models for water in relation to protein hydration, Reidel, Dordrecht, 1981, pp. 331–342.
- 45 B. Chen, J. J. Potoff and J. I. Siepmann, Monte carlo calculations for alcohols and their mixtures with alkanes. transferable potentials for phase equilibria. 5. United-atom description of primary, secondary, and tertiary alcohols, *J. Phys. Chem. B*, 2001, **105**(15), 3093–3104.
- 46 J. M. Stubbs, J. J. Potoff and J. I. Siepmann, Transferable potentials for phase equilibria. 6. United-atom description for ethers, glycols, ketones, and aldehydes, *J. Phys. Chem. B*, 2004, **108**(45), 17596–17605.
- 47 J. M. Martínez and L. Martínez, Packing optimization for automated generation of complex system's initial configurations for molecular dynamics and docking, *J. Comput. Chem.*, 2003, **24**(7), 819–825.
- 48 D. van der Spoel, E. Lindahl, B. Hess, G. Groenhof, A. E. Mark and H. J. C. Berendsen, Gromacs: fast, flexible, and free, *J. Comput. Chem.*, 2005, **26**(16), 1701–1718.
- 49 S. Nose, A molecular dynamics method for simulations in the canonical ensemble, *Mol. Phys.*, 1984, **52**(2), 255–268.
- 50 W. G. Hoover, Canonical dynamics: equilibrium phase-space distributions, *Phys. Rev. A: At., Mol., Opt. Phys.*, 1985, **31**(3), 1695–1697.
- 51 M. Parrinello and A. Rahman, Crystal structure and pair potentials: a molecular-dynamics study, *Phys. Rev. Lett.*, 1980, **45**(14), 1196.
- 52 M. Parrinello and A. Rahman, Polymorphic transitions in single crystals: a new molecular dynamics method, *J. Appl. Phys.*, 1981, **52**(12), 7182.
- 53 J. L. Lebowitz and J. K. Percus, Long-range correlations in a closed system with applications to nonuniform fluids, *Phys. Rev.*, 1961, **122**(6), 1675.
- 54 M. Požar, J.-B. Segulier, J. Guerche, R. Mazighi, L. Zoranić, M. Mijaković, B. Kežić-Lovrinčević, F. Sokolić and A. Perera, Simple and complex disorder in binary mixtures with benzene as a common solvent, *Phys. Chem. Chem. Phys.*, 2015, **17**, 9885–9898.
- 55 A. Perera, L. Zoranić, F. Sokolić and R. Mazighi, A comparative molecular dynamics study of water–methanol and acetone–methanol mixtures, *J. Mol. Liq.*, 2011, **159**, 52–59.
- 56 J.-H. Guo, Y. Luo, A. Augustsson, S. Kashtanov, J.-E. Rubensson, D. K. Shuh, H. Ågren and J. Nordgren, Molecular structure of alcohol–water mixtures, *Phys. Rev. Lett.*, 2003, **91**, 157401.
- 57 R. Ludwig, The structure of liquid methanol, *ChemPhysChem*, 2005, **6**(7), 1369–1375.
- 58 L. Zoranić, F. Sokolić and A. Perera, Microstructure of neat alcohols: a molecular dynamics study, *J. Chem. Phys.*, 2007, **127**(2), 024502.
- 59 M. Požar, B. Lovrinčević, L. Zoranić, T. Primorac, F. Sokolić and A. Perera, Micro-heterogeneity versus clustering in binary mixtures of ethanol with water or alkanes, *Phys. Chem. Chem. Phys.*, 2016, **18**, 23971–23979.

- 60 A. Perera, Charge ordering and scattering pre-peaks in ionic liquids and alcohols, *Phys. Chem. Chem. Phys.*, 2017, **19**, 1062–1073.
- 61 P. Ganguly and N. F. A. van der Vegt, Convergence of sampling Kirkwood–Buff integrals of aqueous solutions with molecular dynamics simulations, *J. Chem. Theory Comput.*, 2013, **9**(3), 1347–1355, PMID: 26587597.
- 62 L. Albuquerque, C. Ventura and R. Goncalves, Refractive indices, densities, and excess properties for binary mixtures containing methanol, ethanol, 1,2-ethanediol, and 2-methoxy-ethanol, *J. Chem. Eng. Data*, 1996, **41**(4), 685–688.
- 63 M. Moosavi and A. A. Rostami, Densities, viscosities, refractive indices, and excess properties of aqueous 1,2-ethanediol, 1,3-propanediol, 1,4-butanediol, and 1,5-pentanediol binary mixtures, *J. Chem. Eng. Data*, 2017, **62**(1), 156–168.
- 64 M. Zaoui-Djelloul-Daouadji, I. Mokbel, I. Bahadur, A. Negadi, J. Jose, D. Ramjugernath, E. E. Ebenso and L. Negadi, Vapor–liquid equilibria, density and sound velocity measurements of (water or methanol or ethanol + 1,3-propanediol) binary systems at different temperatures, *Thermochim. Acta*, 2016, **642**, 111–123.
- 65 J. George and N. V. Sastry, Densities, dynamic viscosities, speeds of sound, and relative permittivities for water + alkanediols (propane-1,2- and -1,3-diol and butane-1,2-, -1,3-, -1,4-, and -2,3-diol) at different temperatures, *J. Chem. Eng. Data*, 2003, **48**, 1529–1539.